Monthly Notices
of the
ROYAL ASTRONOMICAL SOCIETY

Mon. Not. R. Astron. Soc. **412,** 33–48 (2011) doi:10.1111/j.1365-2966.2010.17845.x

Campaign of sky brightness and extinction measurements using a portable CCD camera

Fabio Falchi★

Istituto di Scienza e Tecnologia dell'Inquinamento Luminoso, Via Roma 13, I-36106 Thiene, Italy

Accepted 2010 October 10. Received 2010 July 27; in original form 2010 March 30

ABSTRACT

In this paper, we present the results of a 12-yr campaign devoted to monitoring the sky brightness affected by different levels of light pollution. Different sites characterized by different altitudes and atmospheric transparency have been considered. The standard photometric Johnson *B* and *V* bands were used. An extinction measurement was performed for each site and each night, along with a calibration of the instrument. These measurements have allowed us to build sky brightness maps of the hemisphere above each observing site; each map contains up to 200 data points spread around the sky. We have found a stop in zenith sky brightness growth at the two sites where a time series exists. Using zenith sky brightness measurements taken with and without extensive snow coverage, we weighted the importance of direct versus indirect flux in producing sky glow at several sites.

Key words: light pollution – site testing – techniques: photometric.

1 INTRODUCTION

The brightness of the night sky is one of the most important parameters used to describe the quality of an astronomical site. A series of papers, describing the quality of some Italian sites, was published some years ago (Falchi 1999; Falchi & Cinzano 2000). The sky brightness and extinction measurements taken then have been used to calibrate the first sky brightness map computed from the Defence Meteorological Satellite Programme radiance data (Falchi 1999; Falchi & Cinzano 2000), followed by upgraded models and maps (Cinzano, Falchi & Elvidge 2000, 2001a,b). A continuous monitoring campaign with more sites will allow us to better calibrate the maps of the forthcoming updated World Atlas of artificial sky brightness and the other products published by ISTIL, the Light Pollution Science and Technology Institute.

The campaign of sky brightness measurements presented in this paper was started in 1998 as a thesis work for a master's degree in physics at Milan University (Falchi 1999), and has continued since then. The instrumentation used to obtain the sky brightness and extinction measurements is described in Section 2, and the method of sky brightness measurement is described in Section 3. In Section 4 we report and discuss our results: the selection of observing sites and the brightness and extinction measurements, the all-sky maps obtained from the brightness data, the brightness over the years at two sites, the evaluation of the direct/indirect light in producing sky brightness using data obtained with snow-covered terrain compared with the data taken with no snow.

★E-mail: falchi@lightpollution.it

2 INSTRUMENTATION

The instrument presented here is similar in concept to that presented by Cinzano & Falchi (2003) and to that used by the Night Sky Program of the United States National Park Service (Duriscoe, Luginbuhl & Moore 2007).

The whole instrumentation package had to be easily carried to the sites of observation and had to allow a quick set-up. Portability, ease and speed of the set-up procedure are necessary in order to make it possible to collect more data sets in a single night, at the same site (for different bands or for different times during the night) or at two or more sites. Because of the on-site usage, all the instrumentation should be independent of a 220 V power supply, so a number of 12 V batteries were used to supply the components of the instrumentation: a Microsoft Windows XP based PC, a portable cooled CCD camera, a portable go-to mount. The instrumentation total cost of around 2000 Euros (even less, if assembled from used equipment) should permit the presented method to be used widely in the amateur and professional communities alike.

2.1 CCD camera

The CCD camera had to be small and light so that it could be piloted on a lightweight commercial go-to mount. The camera was piloted via a parallel port from a Windows XP based (Windows 98 for the first years) notebook PC. The selected CCD camera was a Starlight Xpress MX512, because this satisfies all the qualities needed for the campaign. The camera is equipped with a Sony ICX055AL HyperHAD Interline Transfer sensor. The sensor active area is 4.9×3.65 mm^2 distributed on 500×291 pixels. The sensor was chosen for its high quantum efficiency extended into

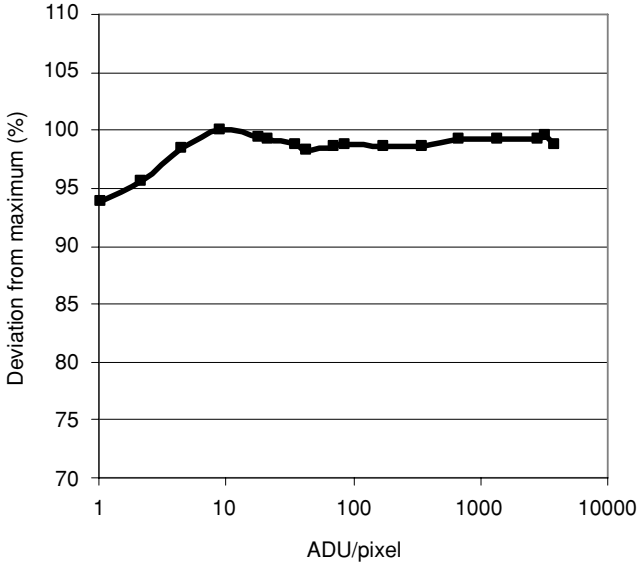

Figure 1. Linearity response of the CCD camera is confirmed up to the saturation level (4096 ADU). Regardless, stars with pixel values of more than 80 per cent of the saturation level were rejected.

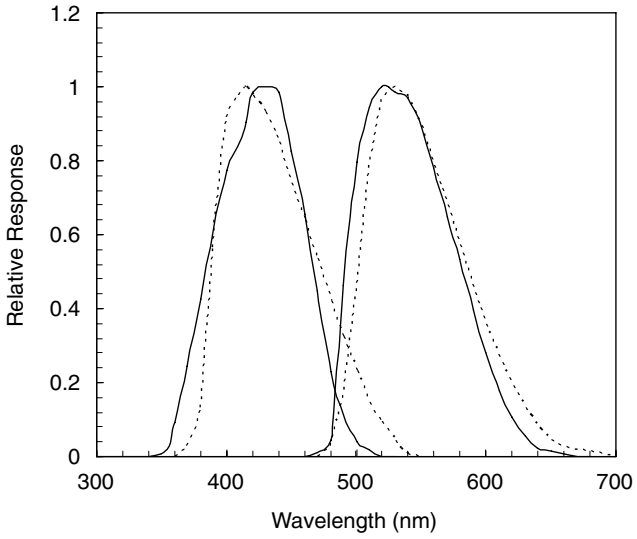

Figure 2. CCD and filter combined quantum efficiency in the *B* band (solid line, left) and *V* band (solid line, right). The dotted lines are the *B* and *V* standard Johnson bands.

the blue portion of the visible spectrum, retaining 70 per cent of its sensitivity at the peak of the *B* band. This blue sensitivity allowed the collection of data in the Johnson *B* band in addition to the *V* band. This sensor has a very low thermal signal, even at the relatively high operation temperature of 30°C below ambient. The linearity of the CCD camera was checked, and it was demonstrated to be very good, up to the saturation level. Anyway, stars with pixel values higher than 80 per cent of the saturation level were omitted from the calibration process. The linearity of the CCD camera was found to be very accurate also at the low ADU values measured in the sky background. In the ADU range used for the calibration stars and the sky background measurements, the deviations from linearity were below ±1.5 per cent, as seen in Fig. 1.

2.2 Filters

Johnson *V* and *B* photometric bands (Johnson 1963; Bessel 1990) were chosen to study the light pollution levels, as done in previous studies (Walker 1970, 1973, 1988; Bertiau, de Graeve & Treanor 1973; Berry 1976; Garstang 1984, 1986, 1987, 1989, 1991; Hoag 1973; Kalinowski, Roosen & Brandt 1975; Krisciunas 1990; Cinzano 1997, 2000a,b, 2003; Falchi 1999; Catanzaro & Catalano 2000; Cinzano et al. 2000, 2001a,b; Falchi & Cinzano 2000; Favero et al. 2000; Piersimoni et al. 2000; Zitelli 2000; Krisciunas et al. 2007; Patat 2003, 2008). This is still the optimal choice. In fact, the *V* band covers well the sensitivity of the human eye in the condition used to observe the starry sky and the *B* band helps to monitor the widespread use of lamps with a strong blue emission (metal halide and white LEDs).

V and *B* photometric filters from Schüler Astro-Imaging were used on the camera. The combined sensitivity curves of these filters and the CCD sensor are shown in Fig. 2. The *B* band has a λ max = 440 nm with a FWHM of 85 nm. The *V* band has a λ max = 530 nm with a FWHM of 95 nm. At 589 nm sodium lamp peak, the CCD with the *V* filter still has 40 per cent of maximum sensitivity. To check the close vicinity to the Johnson standard of the filter + lens + CCD sensor combination, measurements of various colour index stars were performed. The maximum difference of the instrumental magnitude from the standard *B* magnitude is 0.03 mag for stars of *B*–*V* index of more than one. For the great majority of stars, the difference is less than 0.01 mag in the *B* band (Fig. 3, upper plot). The difference between the instrumental *V* magnitude and the standard *V* magnitude is negligible in the *V* band (Fig. 3, lower plot), always under 0.01 mag. For this reason, no adjustment was made for an instrumental colour term.

In both our *B* and *V* bands, the calculated effective wavelengths are shifted toward shorter wavelengths as compared to the standard bands. For the *B* band, our $\lambda_{\rm eff}$ is about 3 nm less than the Johnson *B*. For the *V* band, the difference is larger, about 8 nm. This means that we obtain slightly darker sky values than standard because the natural sky is brighter in the longer wavelength. The difference should be around 0.06 magn in the *V* band for a naturally dark sky and even less in the *B* band. For a polluted sky, the difference with the standard depends on the lamp spectra producing the pollution. For a sky polluted exclusively by high-pressure sodium lamps, the difference should be less than 0.15 mag in the brightest sky measured in our campaign. The presence of bluer light produced by metal halide lamps will lower this difference. For an in-depth analysis of this issue, see Duriscoe et al. (2007).

2.3 Lens

In order to have several non-variable stars of magnitude five or brighter in each frame, we used a fish-eye type lens.

The design of fish-eye lenses minimizes vignetting at the edges while introducing distortions. The CCD dimensions are very small compared to the full 24 × 36 mm^2 frame of the Leica format film for which the lens was designed. Thus, we only used the very central part of the fish-eye field where distortions are almost absent. Of course, the faster the *f*/ratio the better, in order to have short exposures: *f*/2.8 was a good compromise. The chosen optic was a single lens reflex Zenitar 16 mm *f*/2.8 lens. It has a standard 42 mm × 1 mm pitch screw mount, so a simple adapter was used to couple it to the CCD camera. The lens/camera combination allowed a field of view of 16°30′ by 12°10′.

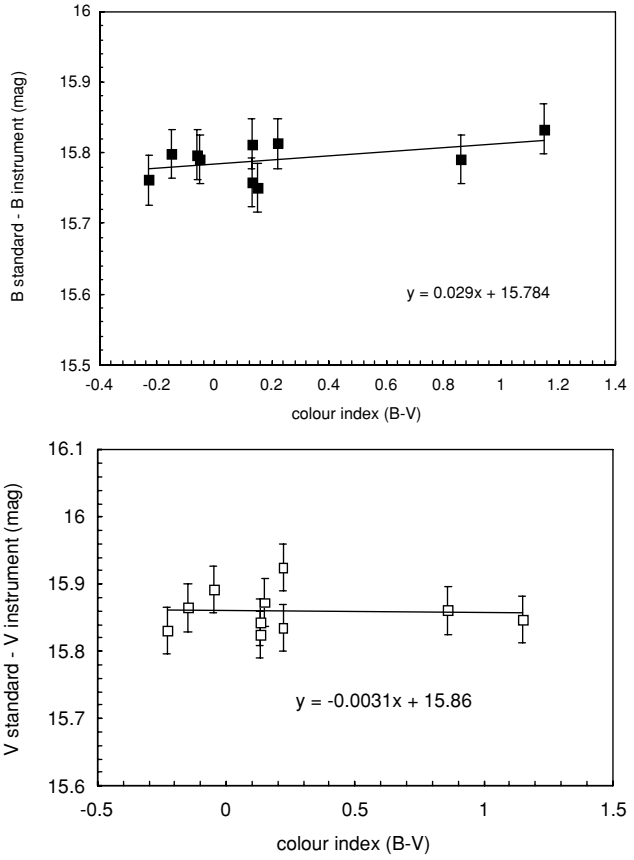

Figure 3. Difference between standard and instrumental magnitudes for the *B* band (solid squares, upper plot) and the *V* band (open squares, lower plot). Error bars were computed by multiple exposures on the same star.

2.4 Mount and control software

The mount used to point the CCD–lens combination was a commercially available alt-azimuth GOTO Celestron NexStar GT mount. A Microsoft Windows XP based (Windows 98 in the beginning) Notebook PC controlled both the CCD camera and its pointing via RS232 and parallel ports. ASTROART 3.0 by MSB Software allowed the creation of scripts that automatically controlled the pointing direction and the exposures of the CCD camera. Both mount and PC can be powered by small 12 V motorbike batteries.

The set-up operations required about half an hour from arrival at the site to the start of data collection.

3 METHOD OF SKY BRIGHTNESS MEASUREMENT

Measurements were performed only during nights of photometric quality (i.e. the ratio between extinction and airmass was constant in the various directions and altitudes from zenith to at least 15° above the horizon). This condition allowed us to be confident that the extinction and atmospheric conditions were constant over a large territory surrounding the observing site. A very low extinction (i.e. high atmospheric transparency) was not required or desirable because the variety of extinction for different nights allows the study of how brightness changes as a function of it. Extinction conditions may also be characteristic of different sites. The first sky brightness measurements were begun after astronomical twilight (with the Sun below 18° under the horizon and the Moon below 10° under the horizon). All these constraints drastically reduced the number of nights available for the measurements, especially in a territory with poor weather such as the Padana Plain where the greater parts of the data sets were collected.

For each set of measurements, a photometric calibration was performed to find the instrumental magnitude constant. Moreover, as a by-product, the calibration procedure gives the extinction coefficient that we need as companion data to the brightness data.

Even if the CCDs usually maintain their stability over time, some other factors may change, such as the transmission of the lens either as a result of the degrading of the antireflection coatings or the dust on the sensor and optics. Regardless, we found that the instrumental magnitude zero point was stable with a value of 8.62 with a standard deviation of 0.08 (0.015 the standard deviation of the mean). A night with a nearly three standard deviation from the mean was rejected. The stars used for the calibration are from the *Hipparcos* catalogue for the *B* band (ESA 1997) and from the Bright Star Catalogue for the *V* band (Hoffleit & Warren 1991). When there was more than one site on the same night, a new calibration was not performed, but it was checked with some standard stars anyway. The images were taken with a slight defocus, in order to have the light from stars falling on more pixels, so increasing the photometric measuring accuracy. The usual FWHM of the measured stars was from two to three pixels. For each calibration, several dozen stars were used, chosen at different azimuth and altitude, paying attention to have several of these at more than 60° elevation and several at less than 30°. On each image, the standard procedure of dark and bias frames subtraction and flat-field correction was used. Master flats were performed using twilight, pointing the camera to a low gradient zone of the sky and making a succession of frames rotating the camera on its axis to eliminate the residual gradient.

To check the overall performance of the camera, we exposed the same area of the sky, pointing the lens toward slightly different directions, in order to have the same spot area of sky in different positions on the sensor from near the centre to the borders. The maximum deviation found was below 0.03 mag, while the standard deviation was 0.01 mag. This test allows us to be confident that the errors as a result of flat-field correction, vignetting and plate scale variations across the field of view are kept below 0.03 mag.

After the explained reduction procedure, the images were ready for the standard star photometry. For each image, usually two or three of the brighter and not variable stars were used, choosing them manually. The ADU counts, obtained with a double circle around the stars (the inner one with the star plus background counts, the outer one with the background counts), were reduced to a 1-s exposure.

For each measured star, the airmass crossed by its light was computed by (Buil 1991)

$$x = \sec z(1 - 0.0012 \tan^2 z), \quad (1)$$

where z is the zenith angle of the star at the middle of exposure. Usually, we used airmass values smaller than 4. The term between brackets is a correction factor significant only for stars at low altitude above the horizon.

Then, we calculated

$$y = m_{\rm cat} + 2.5 \log I_{\rm star}, \quad (2)$$

where $m_{\rm cat}$ is the star magnitude outside our atmosphere and $I_{\rm star}$ is the number of star counts in each second.

Then, we plotted x and y for each measured star (Fig. 4). The best-fitting line gives us both the instrument constant necessary for calibration of the CCD camera–lens–filter combination and the

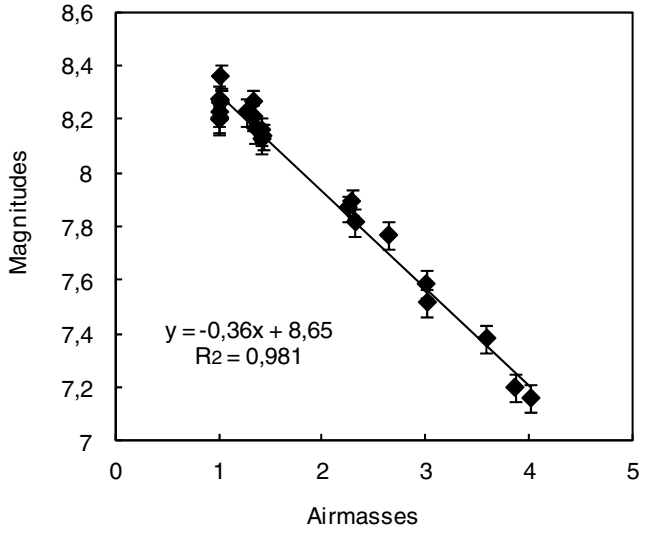

Figure 4. Calibration of a data set in the *V* band for the data taken near Gabbiana (MN) on 2003 September 19. Error bars on stars are computed by linear regression.

extinction coefficient of the sky at the site for that particular night. The intercept gives us the photometric calibration C, while the slope of the line gives us the extinction k in magnitudes per airmass:

$$y = C - kx. \tag{3}$$

This procedure was performed for each data set, *V* and *B*.

Then, we were able to extract the sky brightness from the background counts per second per arcsec^2 ($I_{\rm sky}$). The scale of the CCD image was determined from the astrometric positions of the field stars, both at the centre of the frame and at the border. Each pixel covered an area of sky of 18 800 arcsec^2, which is stable over the field of view because of the geometry of the fish-eye lens design (Rabaza et al. 2010).

Rectangles of about 1 deg^2 were selected manually to compute $I_{\rm sky}$ in order to exclude magnitude 8 and brighter stars. Dimmer stars were left to contribute to the sky background value, as these are not singularly detectable by the human eye and therefore contribute to the natural sky brightness.

The sky brightness in magnitude per arcsec^2 is given by $m_{\rm sky}$:

$$m_{\rm sky} = C - 2.5 \log I_{\rm sky}. \tag{4}$$

This gives us the sky brightness 'under the atmosphere'. This value should not be corrected in order to find the magnitude outside the atmosphere, as usual for astronomical objects, because it will be of no significance for the measurement of sky brightness, almost totally generated inside our atmosphere, both artificially and naturally (Kalinowski et al. 1975; Krisciunas 1990).

The standard deviation of the intercept C was around 0.03 mag in the *V* band and 0.06 in the *B* band. These errors, added squared to the 0.03 mag found in the test mentioned earlier, give us a total error of 0.04 mag in the *V* band and 0.07 in the *B* band.

The sky background brightness measurements were distributed at different zenith angles and azimuths, in order to efficiently cover the celestial hemisphere and, at the same time, to limit the number of necessary exposures. In Table 1, we report the usual pointing directions used in a data set. At some of the sites, the measurements were performed more than once during the night or for the whole night (in the latter cases, only the sky brightness was measured all night long, anyway checking with stars for changes in transparency).

Table 1. Each data set usually has frames centred at the coordinates given in this table. For each frame, the brightness was usually measured at 5° above and below the centre, 7° to the left and right, and near the corners. Altitude is given as 90° minus zenith angle.

Azimuth (deg)	Altitude (deg)
0	15; 30; 45; 60; 75; 90
90	15; 30; 45; 60; 75
180	15; 30; 45; 60; 75
270	15; 30; 45; 60; 75
45	15; 30
135	15; 30
225	15; 30
315	15; 30

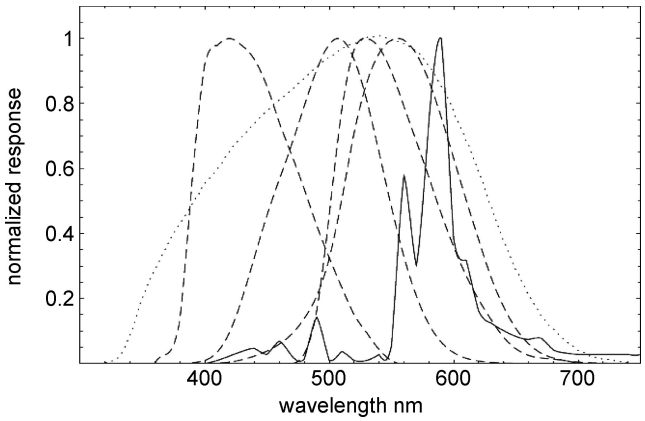

Figure 5. SQM normalized response (dotted line), normalized response of Johnson's *B* band, CIE scotopic, Johnson's *V* band and CIE photopic (dashed lines) and high pressure sodium lamp emission spectra (solid line). (From Cinzano 2005).

A sky quality meter (SQM) or/and SQM-L (a version with a lens and a narrower field of view), from Unihedron was used, in addition to the CCD camera, for several dates and sites. The SQM is a portable photometer that directly gives the sky brightness in mag arcsec^{-2} in a few seconds, simply by pointing it manually directly to the zenith. The spectral response of the SQM is given in Fig. 5. Because of the non-standard passband of the SQM, we calibrated our three SQMs to give the same sky brightness values as our CCD *V*-band measurements at the two sites where we made more CCD measurements: San Benedetto Po and Gabbiana. We have found that our CCD measurements are constantly higher than those of the three SQMs by 0.07, 0.16 and 0.15 mag, respectively. The standard deviation of these differences is less than 0.05 mag. We have also found that consecutive measurements taken with the same SQM pointing in the same direction (by hand) have a standard deviation of 0.02 mag (this is included in the 0.05 error). For our SQMs at the two cited sites, we can confidently measure the sky brightness with the SQM with an error of about 0.06 mag, given by the squared sum with the 0.04 error of the CCD *V* brightness. The SQM could be used to quickly take measurements at several sites. Moreover, when an extinction measurement is available from a CCD data set, the SQM sky brightness measurements in the surroundings of the

CCD measured site can be binned with an extinction measurement, assuming that the extinction has not significantly changed since the CCD extinction measurement.

The manufacturer specification for the accuracy of the SQM is 0.1 mag, and this corresponds to our findings in the differences between the readings given by different SQMs. The error in the reading of the brightness by the same SQM on different nights at the same site can be assumed as 0.05 mag, as specified above.

4 RESULTS AND DISCUSSION

In this section, we analyse some results of the CCD measurement campaign. In Section 4.1, we describe the observing sites and give the brightness and extinction measurements. In Section 4.2, we show the all-sky maps obtained from the brightness data. In Section 4.3, we present the brightness changes over the years. In Section 4.4, we compare the sky brightness data obtained with a snow-covered landscape and streets with the data taken in no-snow conditions.

4.1 Observing sites

The different observing sites were selected so that they have a wide variety of artificial sky brightness, are located in various Italian regions and have different altitudes above sea level.

At the vast majority of the sites, the artificial sky brightness was higher, even several times more, than the natural one. This means that we do not need to worry about the variability of the natural sky brightness as a result of both the diminishing natural airglow during the night (Kalinowski et al. 1975; Walker 1988; Krisciunas 1990) and the presence of zodiacal light and gegenschein. Even the presence of the Milky Way was not detectable in the most polluted sites. None the less, the distance from the Galactic plane was always given in the data reduction spreadsheet when it was lower than 20°.

Each site was at least 1 km away from artificial light sources, except for the sites inside cities. In any case, there were no strong sources near the site (i.e. shopping mall, sport stadium).

In mountain observing sites, artificial sky brightness may significantly vary from night to night, even with a similar measured

Table 2. List of observing sites from the CCD measurement campaign. For data from multiple nights, the brightness and extinction values are the averages. Additional data taken with SQMs are not listed.

Observing site	Latitude N (° ′ ″)	Longitude E (° ′ ″)	Altitude (m)	Date	*B* band		*V* band	
					B brightness (mag arcsec^{-2})	Extinction coefficient (mag airmass^{-1})	*V* brightness (mag arcsec^{-2})	Extinction coefficient (mag airmass^{-1})
San Benedetto Po (MN)	45 3 4	10 55 11	15	15 nights from 1998/08/25 to 2008/11/26	20.97	0.45	20.01	0.31
Gabbiana (MN)	45 6 57	10 37 5	20	18 nights from 2003/09/19 to 2006/10/15	21.24	0.58	20.14	0.34
Mantova (Trincerone)	45 08 10	10 46 58	18	2003/09/21			18.98	
Mantova (Gradaro)	45 08 55	10 48 04	20	1998/11/19	20.25	0.69	18.93	0.38
Mantova (Pontemerlano)	45 06 38	10 52 30	15	1998/11/19	21.26	0.69	20.06	0.38
Pietole (MN)	45 07 48	10 49 00	21	1998/11/19 and 2003/12/24	20.89	0.69	19.60	0.29
Governolo (MN)	45 05 50	10 55 20	15	1998/11/19	21.38	0.69	20.19	0.38
Sustinente (MN)	45 04 04	11 00 04	15	1998/10/14	20.94	0.58	20.08	0.39
Delta Po	44 48 50	12 22 50	1	1999/01/15	22.14	0.46	21.20	0.31
Isola del Giglio	42 20 20	10 54 10	250	1999/09/10 and 1999/09/12	22.77	0.62	21.73	0.36
Modena	44 40 33	10 54 30	35	1998/11/17	19.97	0.37	18.93	0.24
Modena Villanova	44 41 30	10 56 10	30	1998/11/17	20.32	0.37	19.4	0.24
Soliera (Modena)	44 43 15	10 57 58	30	1998/11/17	20.8	0.37	19.92	0.24
Verona	45 23 17	10 58 02	50	1998/11/20	19.48	0.51	18.43	0.34
Bigliana di Gualtieri (RE)	44 51 08	10 35 46	18	2004/05/18			19.89	0.41
Folgaria (TN)	45 53 29	11 12 04	1606	2004/08/14			21.07	0.14
Musiara (PR)	44 29 46	10 10 25	1070	2004/08/18			20.98	0.25
Murci (GR)	42 45 40	11 22 03	110	2004/09/05 and 2004/09/06	22.30	0.50	21.39	0.34
Tatti (GR)	43 02 26	11 01 05	540	2006/08/27 and 2006/08/30			21.49	0.23
Campo Catino (FR)	41 49 18	13 19 45	1500	2005/09/01 and 2008/08/29	21.34	0.66	20.98	0.47
Cima Ekar (VI)	45 50 56	11 34 08	1366	2001/07/21 and 2001/07/22			21.07	0.19

extinction coefficient. This is because, even if we observe the same transparency above the site, the transparency of the atmosphere above the sources at a lower elevation may be quite different: one night there may be tenuous fog that diffuses more of the light, causing a higher luminance at the site, or, in contrast, there may be clouds that partially screen the towns below the site, diminishing the measured sky brightness.

At sites near sea level, these effects should be more limited. In fact, the extinction measured at the site should be approximately the same extinction experienced by the light leaving the pollution sources around the site. Of course, the further away the sources are from the site, the more the extinction could be different from that measured.

In Table 2 we list the sites along with the *B*- and *V*-band brightness and extinction. The reported data are averaged when more than one night was used. The brightest measured site is near Verona, which gave 18.44 mag arcsec^{-2} in the *V* band. The darkest site is in Giglio Island, with a *V*-band brightness of 21.73 mag arcsec^{-2}.

At the two sites where multiple measurements were made, we searched for a correlation with the hour of the night and with the season (see Section 4.3.1). A correlation with the atmosphere transparency was also investigated (see Fig. 6). In the range between 0.18 and 0.55 mag airmass^{-1}, no significant correlation was found at either site. On an exceptionally hazy night (exceptional for being measured, not for the frequency of these nights in the Padana Plain) with a 1.5 mag airmass^{-1}, we found a significantly darker sky in San Benedetto Po.

4.2 All-sky maps

The observing technique was designed to obtain photometry of the selected points in such a way as to cover as uniformly as possible the entire sky and to avoid in the selected areas the presence of stars brighter than magnitude 8. This choice was made to avoid the contamination of bright starlight, but also to retain the natural

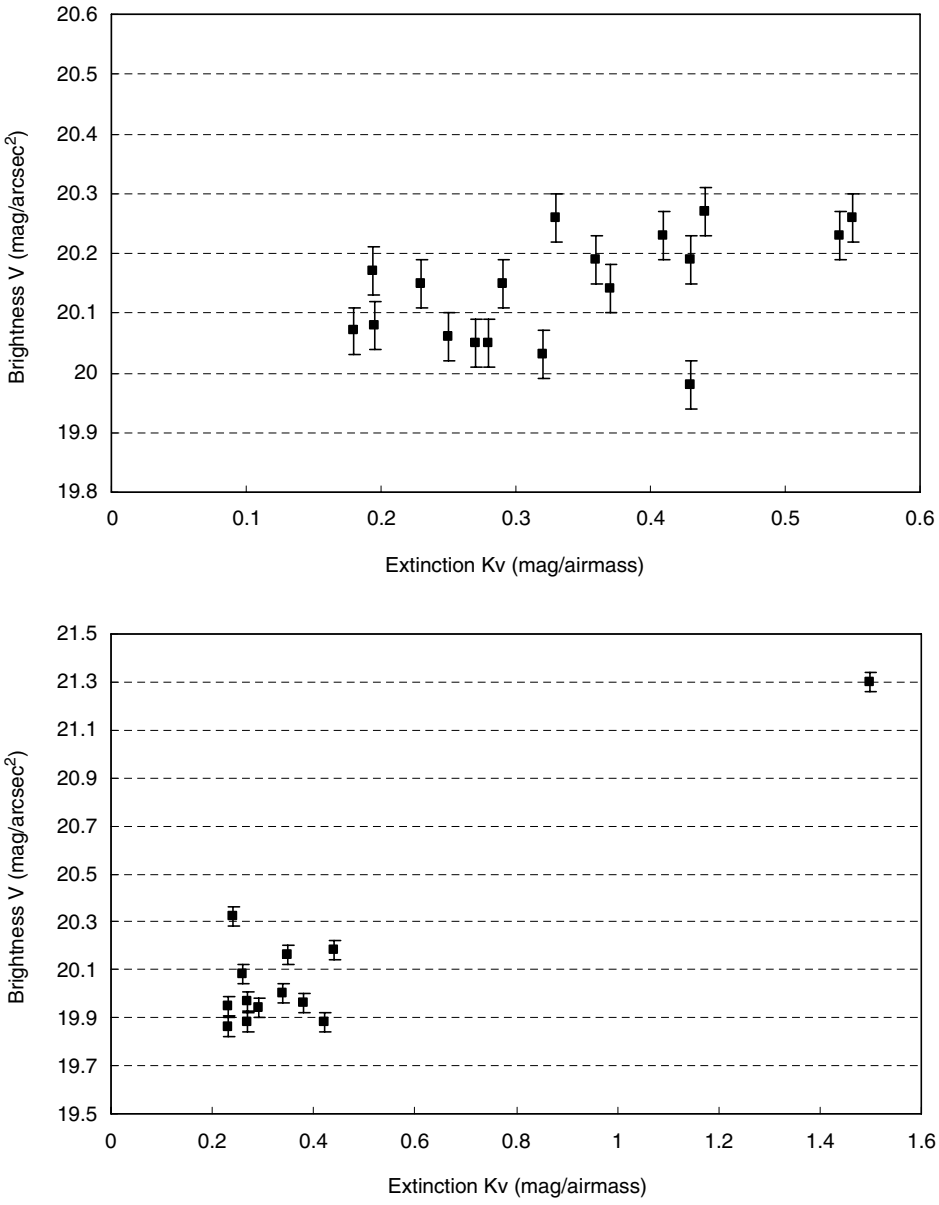

Figure 6. *V* band brightness versus extinction at Gabbiana (upper plot) and San Benedetto Po (lower plot).

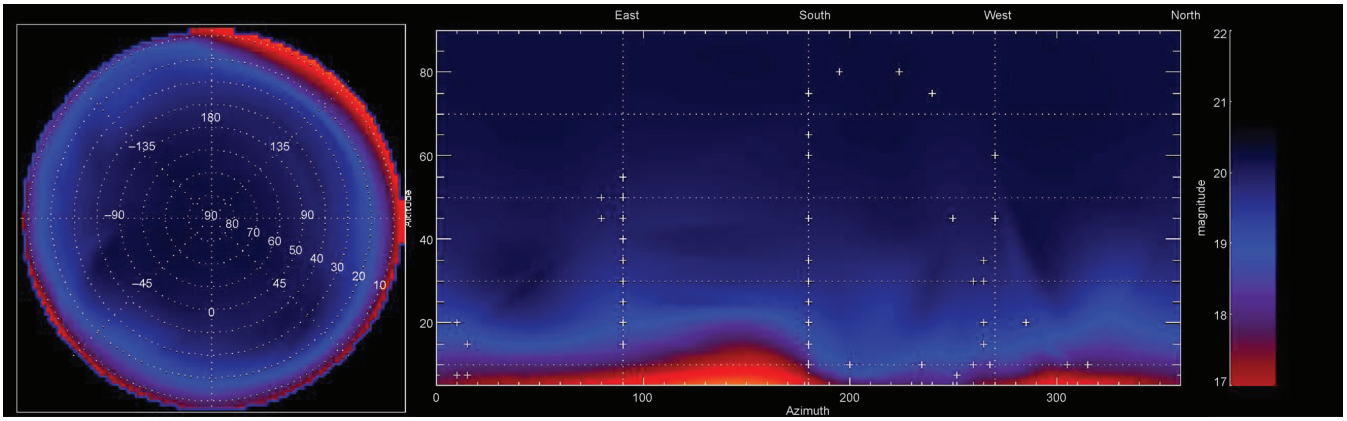

Figure 7. Example of an all-sky map obtained from a set of measurements taken at Gabbiana. This site has a zenith sky brightness of around 20.1 mag arcsec^{-2}. Some interpolation artefacts are a result of the undersampling of sky brightness data points used. Crosses represent where the sky brightness measurements were taken.

contribution of unresolved stars above the naked eye limiting magnitude that contributes to the natural sky background. The usual altitude and azimuth coordinate centres of the frames of the sky used in the data sets are shown in Table 1.

The maps shown in Figs 7 and 8 have been made by Giovanni Catanzaro by means of an interpolating procedure created in the IDL environment (Catanzaro & Catalano 2000). These maps describe the trend of the night brightness in mag arcsec^{-2}. Azimuth coordinates are measured in degrees from the north point eastwards (i.e. east is at 90°, south at 180°, west at 270°). Some interpolation artefacts are present, because of the undersampling of sky brightness data points used. For future works, the number of points will be increased.

These all-sky maps could also help us to find a sky quality indicator other than the brightness at zenith, such as the mean sky brightness at above 15° altitude or the illuminance on the ground by the night sky. These indicators could be useful in addition to the zenith sky brightness, as the zenith is usually the location in the night sky least affected by the detrimental effect of light pollution.

4.3 Brightness versus time

4.3.1 Results of the time series

The first photometric data were collected by our group at several different sites in 1998 (Falchi 1999). For two sites, San Benedetto Po Observatory and Gabbiana, the data were collected on a regular basis, and now there are two time series for these sites (see Figs 9 and 10). The time series shows a constant zenith sky brightness over time in both the 5-yr time series of Gabbiana and the 12-yr time series of the San Benedetto Po Observatory.

We searched for seasonal trends in order to find evidence of influences (e.g. the presence or not of foliage on trees, which could screen the light produced). No particular seasonal trends were detected, even if a higher number of observations were needed to be certain of excluding the possibility of such trends.

The analysis of the sky brightness during the night showed a slight decrease of around 0.2–0.3 mag darker from the early hours (7 or 8 pm) to 11 pm or midnight (Fig. 11). After midnight, the sky brightness seems to be constant, with sometimes a very slight (0.1–0.2) increment later than 2 or 3 am shown on the nights when continuous monitoring was performed.

4.3.2 Discussion of the time series

As seen, we detected a stasis of the zenith sky brightness at the San Benedetto and Gabbiana sites. This is an unexpected finding because several previous works found an annual increase in artificial sky brightness, usually between 5 and 10 per cent, in all the developed countries studied (Walker 1991; Isobe & Hamamura 1999; Cinzano 2000b, 2003; Hanel 2000; Garstang 2004). Fig. 12 shows the measurements at San Benedetto Po Observatory along

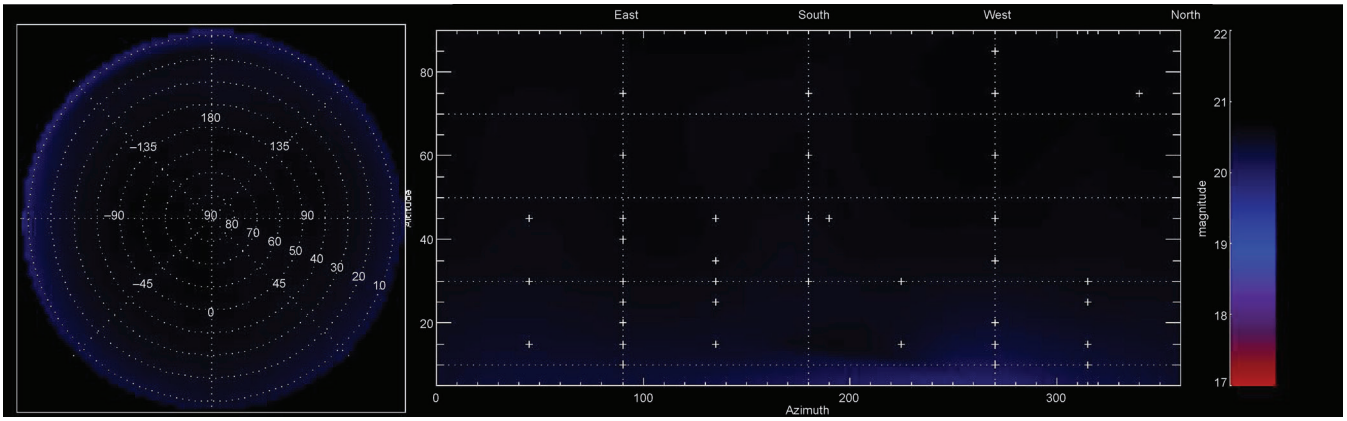

Figure 8. The Poggio al Toro site, near Murci, represented with the same scale as Fig. 7. This is a relatively unpolluted site with a zenith sky brightness of around 21.4 mag arcsec^{-2}. Some interpolation artefacts are a result of the undersampling of sky brightness data points used.

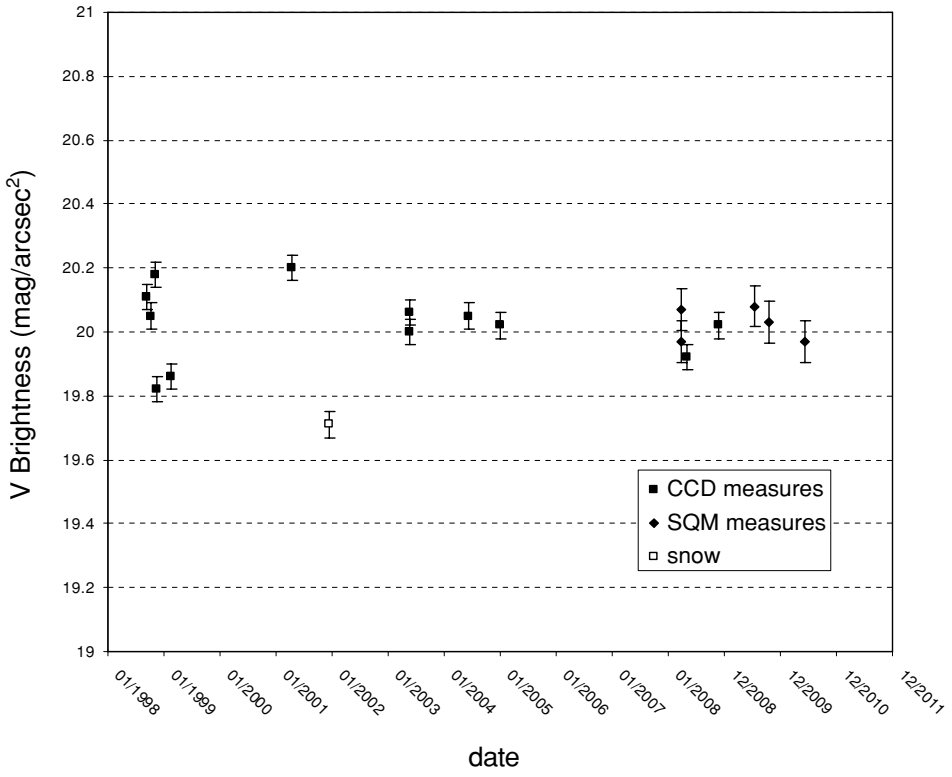

Figure 9. Total sky zenith *V*-band brightness at San Benedetto Po Observatory from 1998 to 2010. The data represented by open squares were taken with a snow-covered landscape (19.71 mag). The solid diamonds denote measurements taken with calibrated SQMs (see text for details).

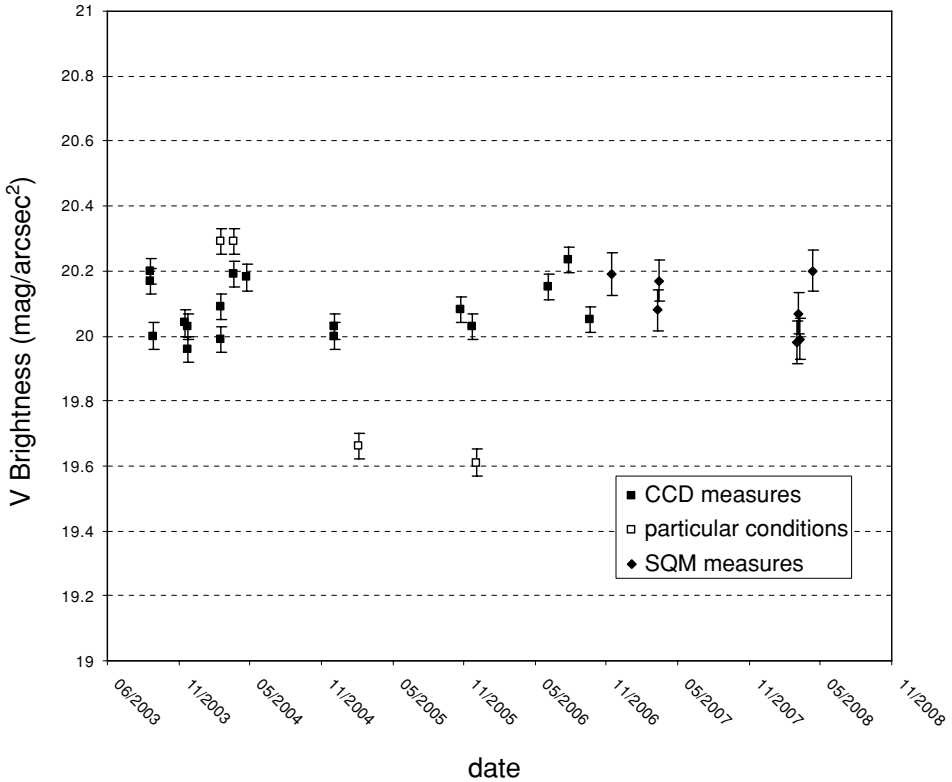

Figure 10. Total sky brightness in Gabbiana from 2003 to 2008. The data represented by open squares were taken in particular conditions: late at night (the two with 20.3 mag), and with a snow-covered landscape (19.65 and 19.60 mag). The diamonds denote measurements taken with calibrated SQMs (see text for details).

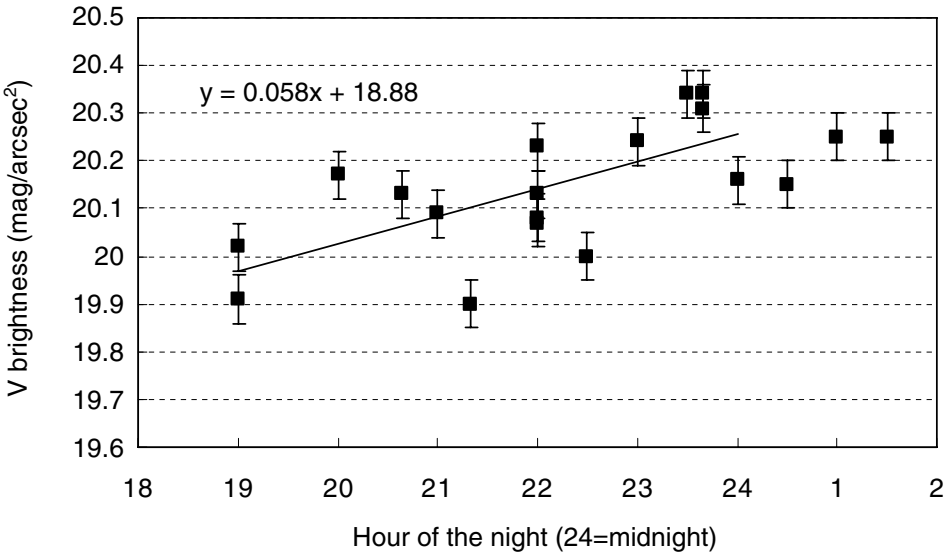

Figure 11. The *V* brightness at zenith at Gabbiana plotted against the hour of the night. The linear regression is calculated excluding the three points after midnight.

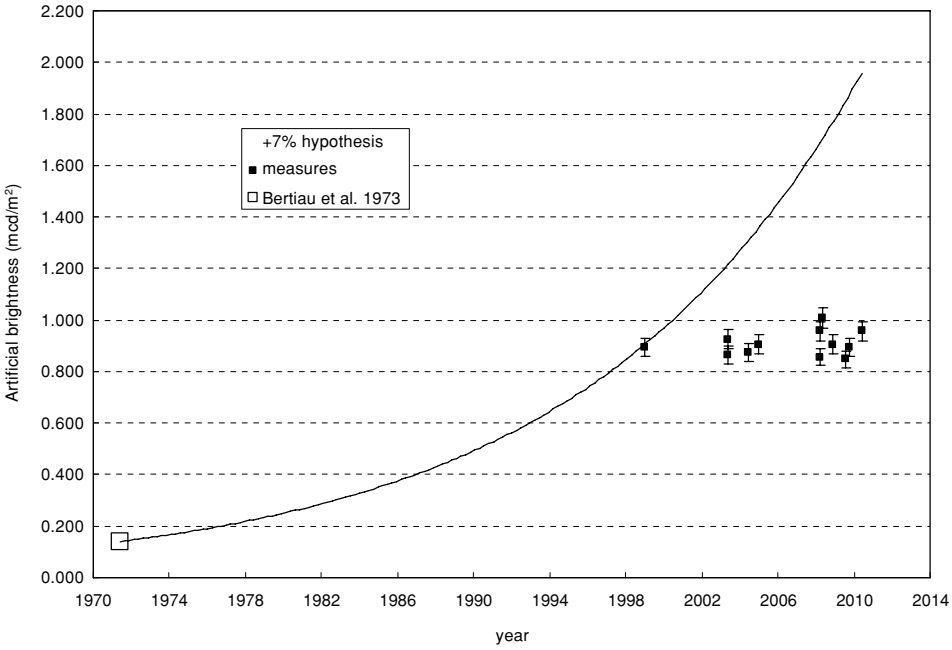

Figure 12. Artificial sky luminance derived from *V*-band measurements at zenith at San Benedetto Po Observatory from 1998 to 2010. The line is a +7 per cent yearly growth constrained to meet the Bertiau et al. (1973) estimate (large open square) and the first CCD brightness data (in 1998).

with the Bertiau et al. (1973) estimate of artificial brightness for the site in 1971. An exponential growth of artificial sky brightness was found by Cinzano in the Veneto region from 1960 to 1995 (Cinzano 2000b). Veneto is a nearby region with the same development, income, lighting habits and productive structure as that where the two sites are located. Moreover, the two sites are also polluted by the lights of Veneto, so, at least in part, the growth of the illumination in Veneto should have reflected in a growth in the sky brightness at the two sites. An analysis of the electric energy consumption in public lighting during the years in the three regions surrounding the sites shows a 140 per cent increase in a 27-yr span, from 1971 to 1998, corresponding to an annual increase of 3.3 per cent (Fig. 13). Unfortunately, the data for each region are available only since 1977, so we have used the data for Italy in the years from 1971 to 1976 to obtain a good estimation of the consumption of the three regions. The emitted light flux has surely increased more than the energy usage, because of the growth in the mean efficiency of the installed lamps. In the early 1970s, a significant number of the lights used outdoors were of incandescent type and mercury vapour lamps had not yet saturated the market then. Assuming a 1971 mean efficiency of 30–40 lm W^{-1} compared to 69 lm W^{-1} in 1998 (Regione Lombardia 2003), we can expect four to five times more light flux in

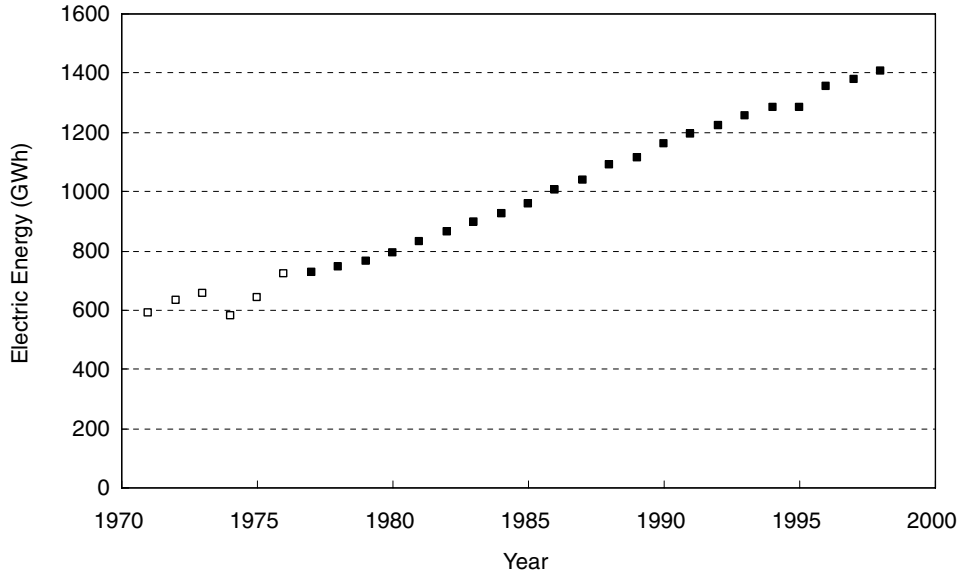

Figure 13. Electric energy consumption as a result of public lighting in the three regions, Lombardia, Emilia-Romagna and Veneto, surrounding the Gabbiana and San Benedetto Po sites. Solid squares denote the sum of the energy usage of the three regions while the open squares are obtained from data from the whole of Italy. Data taken from Terna S.p.A. (http://www.terna.it/Default.aspx?tabid=419).

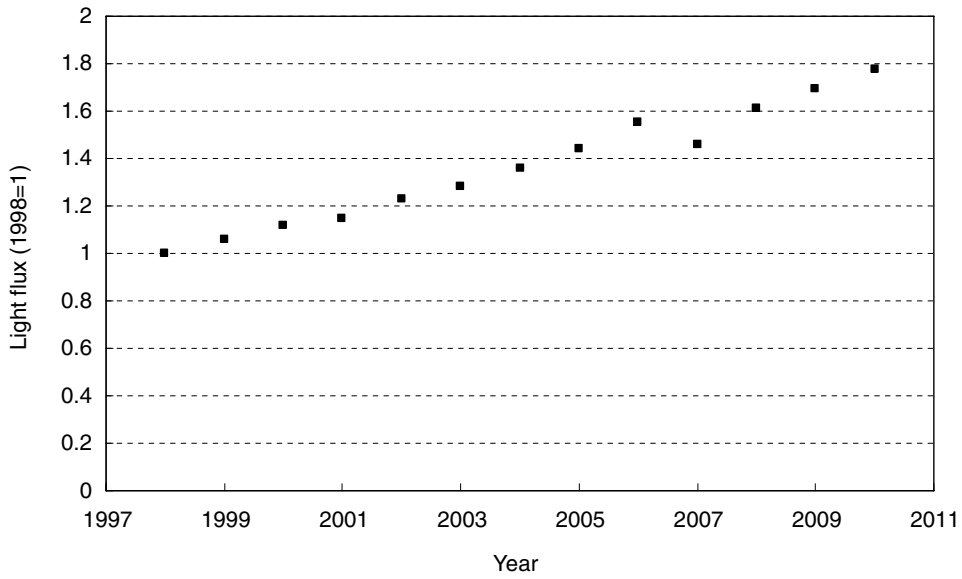

Figure 14. Increase in the installed flux in the regions surrounding San Benedetto Po calculated from the public lighting energy consumption and efficiency of the installed lamps.

1998, compared to 1971. So we can expect an exponential increase in the sky brightness at the two sites. The solid line in Fig. 12 shows an exponential growth constrained to fit the two points of 1971 and 1998. A +7 per cent yearly growth fits the points. The same growth extrapolated to 2010 should have given almost a doubling in artificial sky brightness since 1998. This extrapolated increase of the sky brightness is also supported by the increase in energy consumption from 1998 to 2010 and the increase in the mean installed efficiency. The energy used for public lighting in the three considered regions increased from 1407 GWh in 1998 to 1803 GWh in 2008 (the last available year). The mean efficiency in 1998 can be assumed equal to 69 lm W^{-1} (Regione Lombardia 2003). Considering an efficiency of 100 lm W^{-1} in all the new installations (given by the energy increase) and an equal substitution of old inefficient installations, we arrive at the 80 per cent increase of the installed flux illustrated in Fig. 14, where the 2009 and 2010 data have been extrapolated.

The data on both energy usage for public lighting and the efficiency of the installed lamps imply that we should have expected a growth in the sky brightness from 1998 to now. Instead, we have detected a stasis of the zenith artificial sky brightness, which likely appears to be the result of a change in lighting habits. In fact, several light pollution laws have been enforced in the surroundings of the sites since 1997. The Lombardia region, where the two sites are located, adopted an effective light pollution law in 2000 March. This law, addressing all the new installations, does not allow for direct emissions above the horizon plane from the fixtures, limits

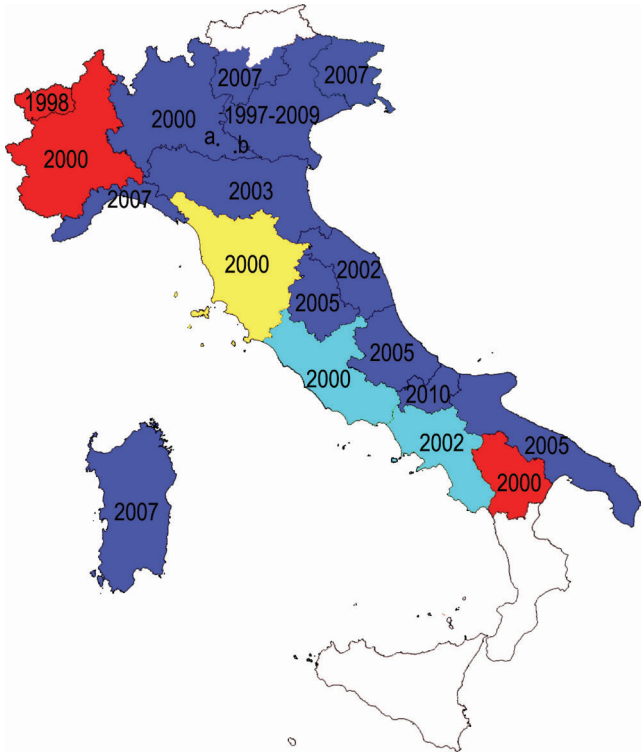

Figure 15. The Italian regional laws against light pollution are shown, along with the year of adoption. The regions with zero direct upward flux are shown in blue. Laws with zero direct upward flux with some limited exceptions are shown in light blue. An allowed 3 per cent upward flux is shown in yellow. Laws with even higher limits or no technical prescriptions are shown in red. Regions without laws are shown in white. Veneto, the first region to adopt a law in 1997 with a 3 per cent allowed flux, upgraded its law to a zero upward flux in 2009. Points a and b are the Gabbiana and San Benedetto Po sites, respectively.

the lighting levels, prescribes some adaptation and retrofitting for the old fixtures and is effective on both private and public lighting. As shown, in the last 10 yr, a 70 per cent growth in installed light flux should have been expected from the increase in public lighting energy consumption, the numerous new public and private installations and the increase in installed lamp efficiency. This increase in installed light flux is not mirrored in an increase of the artificial sky brightness very likely because of the good effect of not allowing for new upward direct emissions and because of the conversion to fully shielded of several old fixtures. Several cities now have only fully shielded fixtures. The lack of growth in sky brightness is a well-deserved success for people belonging to associations such as CieloBuio, who have been fighting this type of pollution. Their efforts secured the enforcement of laws against light pollution in the three regions surrounding the two observing sites (Lombardia, Emilia-Romagna and Veneto regions). Other laws have followed, and now most of Italy is more or less protected from runaway light pollution (Fig. 15).

4.4 Direct versus indirect flux with snow

4.4.1 Method

The zenith sky brightness measurements taken with snow coverage, compared to similar measurements taken in the same places without snow, allow us to separate the fraction of the sky luminance as a result of direct light emitted by the fixtures (including the very small part resulting from signs and billboards) and the fraction as a result of light reflected by the terrain. In fact, the direct flux remains the same, while the reflected flux increases because of the snow coverage. A negligible part of the light escaping upward, not directly coming from fixtures, and not affected by snow is that reflected by vertical surfaces, such as house walls, and that escaping from windows. The latter is absolutely small in magnitude[1] and more so because in Italy during winter most windows are closed after sunset to help keep warmth inside homes. The former may seem not negligible at first sight, but its magnitude is small in any case[2] and it depends on the type of fixture: a fully shielded fixture illuminates far less the surrounding vertical surfaces than a partly shielded fixture or a fixture that is not shielded. So, even the vertical surfaces not affected by snow 'work' to produce low-angle upward light if the fixtures used are not fully shielded, and much less if such reflected light is produced by fully shielded fixtures.

Snow reflects approximately 60–80 per cent of light hitting it, with a higher value for fresh snow. Moreover, it reflects back to the sky the light coming from the polluted sky. The reflection of artificial sky light by snow on the countryside could noticeably enhance the upward flux in polluted areas, such as the sites measured. With the extinction measured at two of the sites (0.5 mag airmass^{-1}) roughly 15 per cent of the upward flux is scattered downward by atmospheric particles and molecules, and 70 per cent of it is reflected upward again by the snow-covered terrain. The increase of artificial sky brightness because of multiple back-and-forth reflections on the snow of sky light is about 10 per cent more than when the landscape is not covered by snow. Table 3 lists the assumptions used to compute the effect of direct versus reflected light on sky luminance.

Solving the system below gives us the fraction of sky brightness as a result of direct and indirect light:

$$d + i = 1$$

$$d + bi = \frac{m_s}{m_0}.$$

Here, d is the fraction of sky luminance as a result of light coming directly from fixtures, i is the fraction as a result of reflections, b is the 'boost factor' as a result of the snow, m_s is the measured brightness with snow (minus the fraction resulting from multiple landscape–sky reflections) and m_0 is the usual brightness without

[1] A 'Fermi problem' quick answer to this is the following. The per capita public lighting flux is about 1500–2000 lm (from 1800 GWh, 80 lm W^{-1} efficiency, 19.1 million inhabitants of the three regions). We calculate the per capita flux escaping from windows in the following way. Typical families have three members and one lighted room at a time. Flux produced inside a typical (5 × 4 m^2 and 3 m high) room: 1500 lm. Mean illuminance on the floor and walls: 16 lux. Flux diffused by these surfaces (reflectance 0.3): 5 lumen in each square metre. Flux escaping from a 2 m^2 window after reflection from walls or floor (not directly from lamps because usually the higher border of the window is lower than the light source and the source is upward screened): 10 lm per family. Flux per person is about 3 lm.

[2] Here is an estimate of the flux reflected by houses. In a typical street, the houses (road 10 m wide, front house distance 20 m, average distance from street light 10 m) have an illuminance of 0.5 lux. The front area of a family house: 75 m^2. Area per capita: 25 m^2. Albedo of the walls: 0.3. Reflected flux per capita: 4 lm. Of this flux, half is downward. Moreover, most Italians live in jointly owned buildings, so the building wall area per capita is even less than assumed.

Table 3. Assumed values for the computation of direct versus reflected effect on sky luminance. The reflectance assumed for roads was that of a 3-yr-old asphalt, 8 per cent at 540 nm (Herold & Roberts 2005). $F_0 = 1 - F_r$. In the formulae, both terms were maintained for clarity.

Assumption	
Fraction of downward flux on roads (F_r)	0.35 ± 0.05
Fraction of downward flux off streets (F_o)*	0.65 ± 0.05
Reflection of roads (R_r)	0.08 ± 0.02
Reflection of surroundings (R_o)	0.15 ± 0.03
Reflection of surrounding with snow (R_{snow})	0.7 ± 0.1
Reflection of roads with snow ($R_{roads\,snow}$)	0.5 ± 0.1
Fraction of roads still covered with snow (F_{rs}):	0 at Gabbiana (2005 March)
	0.10 ± 0.05 at Tradate and Cembrano (2009 December)
	0.20 ± 0.07 at Osteria Grande (2009 December)
	0.3 ± 0.1 at San Benedetto Po (2001 December)
	0.5 ± 0.1 at Zaplana (2009 December)
Fraction of surrounding of streets	0.5 ± 0.1 at Gabbiana (2005 March)
(walkways, grass fields, gardens) with snow (F_{ss}):	0.8 ± 0.2 at Cembrano (2009 December)
	0.9 ± 0.1 at San Benedetto Po (2001 December)
	1.0 ± 0.2 at Tradate, Osteria Grande and Zaplana (2009 December)

snow. The boost factor b is the ratio between the reflected upward flux with snow and that reflected without snow:[3]

$$b = \{F_r [R_r (1 - F_{rs}) + R_{roads\,snow} F_{rs}] + F_o R_{snow} F_{ss} + F_o R_o (1 - F_{ss})\} (F_r R_r + F_o R_o)^{-1}.$$

Here, the symbols are those given in Table 3.

The fraction d of the artificial sky brightness as a result of direct light should be

$$d = \frac{(m_s/m_0) - b}{1 - b}.$$

4.4.2 Results

At two sites we performed CCD sky brightness measurements shortly after a snowfall event covering all the surroundings of the sites, for several tens of kilometres at least, as checked by satellite data (Figs 16 and 17). This check showed that, on an additional third night, the surroundings were not as snow-covered as it seemed when examining near to the site only; so, the measure taken on that night was rejected. For the observation of 2001 December, the satellite image was taken the day after the sky brightness measure and some snow probably melted in the time between the measure and the moment the satellite image was taken. We checked ground-based records of the snow coverage, which confirmed that there was much more coverage than that shown in the image on the following day (Centro Geofisico Prealpino, private communication). Anyway, even if the snow coverage was limited to that shown in the image, none the less the snow-covered area comprised more than 90 per cent of the contribution of light sources producing the zenith sky brightness at San Benedetto Po (Cinzano 2000a). We also used data from four additional sites collected with SQMs by Lorenzo Comolli (Tradate, Italy), Francesco Giubbilini (Osteria Grande, Italy) and Paolo Pescatori (Cembrano, Italy) and with a CCD camera by Andrej Mohar (Zaplana, Slovenja) shortly after a large snow storm in central Europe in 2009 December (Table 4 and Fig. 18).

We found an increase of sky brightness, but it is small, considering that snow reflects light about 10 times more than road asphalt. As seen in Table 5 and Fig. 19, the light that produces most artificial sky brightness, at all sites, is light escaping directly from fixtures.

4.4.3 Discussion

The differences in the direct/reflected ratio between sites may be explained by the different distances from the primary sources producing skyglow (Cinzano & Castro 2000), by the different coverage of the snow and our evaluation of it, by the different extinction factors and the different shape in the upward flux function of the sources around the sites.

The two sites with lower ratios have a contribution of direct flux of about 60 per cent and are very near to or embedded in the major sources of light pollution. Zaplana is 22 km west of Ljubljana, which has 270 000 inhabitants and is the biggest source of light pollution in Slovenja. The Tradate site is inside a village with 15 000 inhabitants, 11 km from a town with 80 000 inhabitants and 35 km from the centre of Milan. In these conditions, inside or very near cities, the reflected light is a large contributor to the production of artificial sky brightness.

The sites with the highest contribution of direct light are San Benedetto Po and Cembrano, with more than 90 per cent. At both sites, the measurements with snow were taken shortly after a law against light pollution was adopted in these regions, so the imposed limits to the direct light could not have a significant effect. Both sites (especially Cembrano) are located far away from large cities, and so their skies seem to be lighted primarily by light escaping directly from fixtures. For San Benedetto Po, the lights polluting its sky have now substantially changed to fully shielded, even if many private lights (industries, factories, deposits, farms, gardens, homes) have yet to be converted. This change in lighting habits should be reflected in the direct/reflected ratio. In order to check this, we are waiting for another snow storm, followed by a clear night. The measurements at Gabbiana, which is a site similar to San Benedetto Po as far as the surrounding pollution sources are concerned, were taken five years after the enforcement of the Lombardia law against light pollution. This law greatly reduces (setting to zero) the direct

[3] If streets are completely clear of snow, the boost factor can be simplified to

$$b = \frac{F_r R_r + F_o R_{snow} F_{ss} + F_o R_o (1 - F_{ss})}{F_r R_r + F_o R_o}.$$

Figure 16. Image of northern Italy taken on 2001 December 16, the day after the measurement taken at San Benedetto Po Observatory, the position of which is indicated by 'X'. (NASA/GSFC, MODIS Rapid Response).

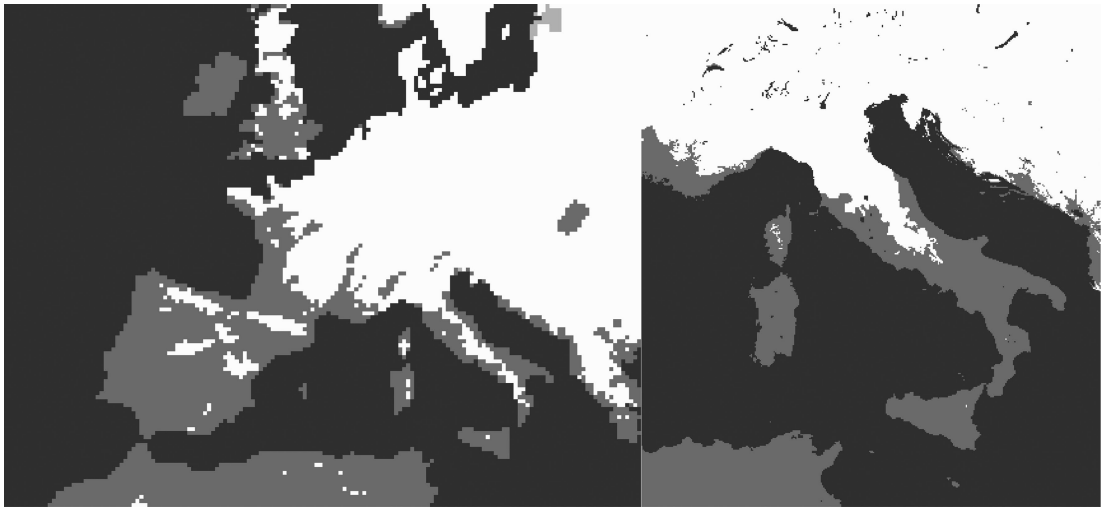

Figure 17. Snow coverage at 24 km resolution on 2005 March 4 (left). Snow coverage at 4 km resolution on 2009 December 20 (right). (NOAA/NESDIS/OSDPD/SSD. 2004, updated 2006. IMS daily Northern hemisphere snow and ice analysis at 4 and 24 km resolution. National Snow and Ice Data Center, Boulder, CO. Digital media.)

Table 4. Sites used for snow measurements in 2009 December.

Observing site	Latitude N (° ′ ″)	Longitude E (° ′ ″)	Altitude (m)	Observer
Tradate	45 42 44	8 54 26	305	Lorenzo Comolli
Osteria Grande	44 25 17	11 32 3	60	Francesco Giubbilini
Cembrano	44 21 31	9 35 38	340	Paolo Pescatori
Zaplana	45 59 10	14 13 45	670	Andrej Mohar

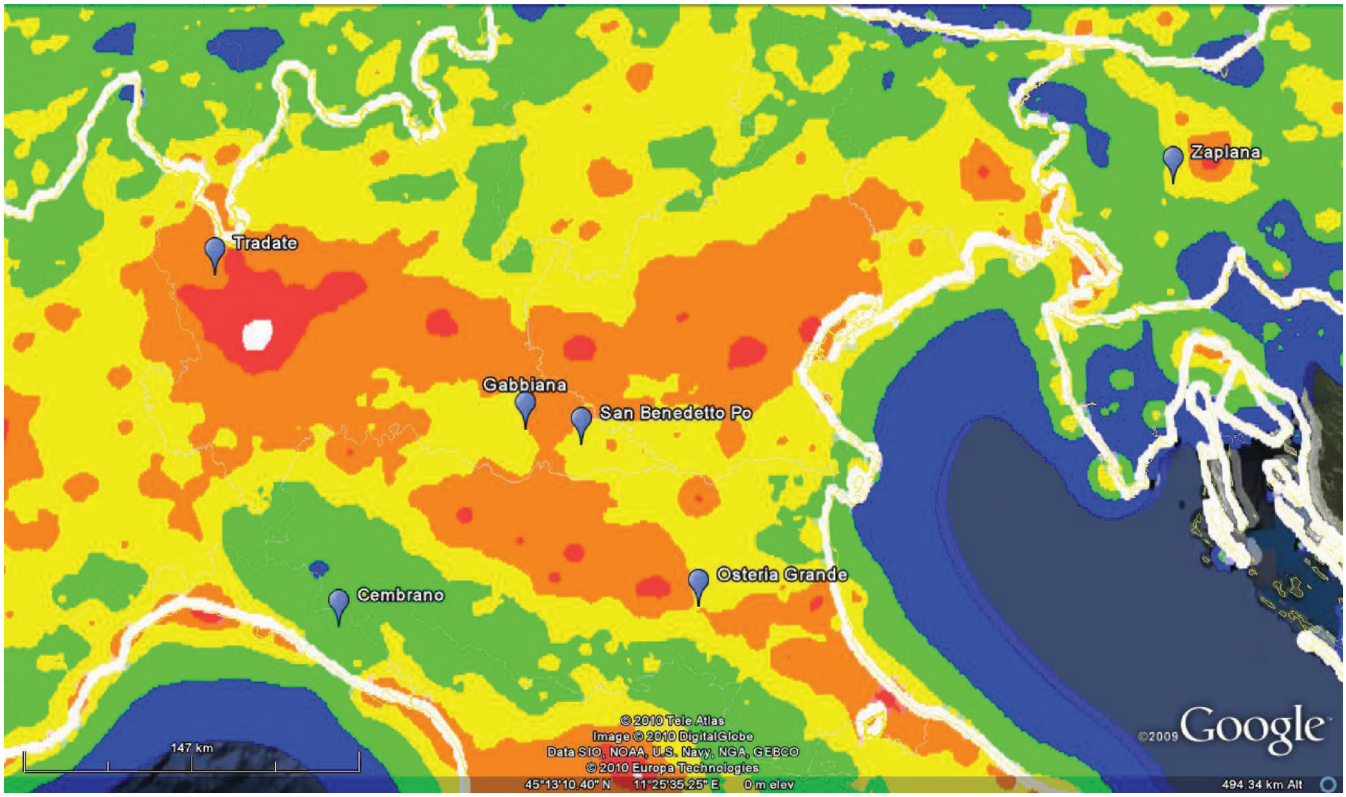

Figure 18. Maps of the six sites used in the snow study. Superimposed on to the Google™ map is the artificial sky brightness map of the First Atlas of Artificial Sky Brightness (Cinzano et al. 2001a). The blue, green, yellow, orange, red and white colours indicate 0.11–0.33, 0.33–1, 1–3, 3–9, 9–27 and more than 27 times the natural night-sky brightness, respectively.

Table 5. Measured brightness with snow and direct versus reflected light efficiency in producing sky luminance at the two sites. An error of 0.05 mag was assumed for the 'usual brightness' at San Benedetto Po and Gabbiana (where numerous nights were used), while an error of 0.1 mag was assumed for the sky brightness with snow coverage and for the other sites 'usual brightness'.

Site	Date	Observed ratio of artificial brightness to usual brightness[a]	Extinction coefficient of the snow measure (mag airmass^{-1})	Fraction of sky brightness due to direct light	Ratio direct/ reflected
San Benedetto Po	2001/12/15	1.31	0.58	0.94 ± 0.04	16
Gabbiana	2005/03/04	1.62	0.51	0.68 ± 0.14	2.1
Cembrano	2009/12/19	1.3	Not measured	0.92 ± 0.07	12
Osteria Grande	2009/12/19	2.0	Not measured	0.74 ± 0.11	2.8
Tradate	2009/12/19	2.4	Not measured	0.61 ± 0.15	1.5
Zaplana	2009/12/20	2.6	Not measured	0.60 ± 0.15	1.5

[a]Before the 10 per cent subtraction made because of the multiple landscape–sky reflections.

emissions from fixtures in all new installations and also prescribes some modifications to old installations. Thus, the direct flux polluting the sky at Gabbiana could already have been reduced in 2005, and perhaps the direct/reflected ratio is lower than that of the San Benedetto Po Observatory partly for this reason.

Even the two sites with a higher direct/reflected ratio are in a relatively densely populated areas in northern Italy, with many small villages a few kilometres from one another (especially San Benedetto Po). In countries with a different distribution of villages, we can expect an even higher ratio in sites further away from the sources of light pollution. At these sites, the suppression of the direct contribution to artificial sky brightness may well restore the night sky to levels of artificial sky brightness 10 times or less than now. Inside cities, the benefits of fully shielded lights will be far less evident in the sky but will anyway be of great benefit to citizens because of a reduction in obtrusive light and glare. Additional measures should be enforced to maintain the reduction in years to come, such as limits to installed flux (and even a reduction of this, of course), limits to the switch-on time of some lighting installations, and the protection of some health-sensitive and environmentally sensitive light bands.

An examination of the manufacturer photometrics of commonly used poorly shielded outdoor lights, such as prismatic-type fixtures, shows that direct uplight is only a few per cent of total output, and in

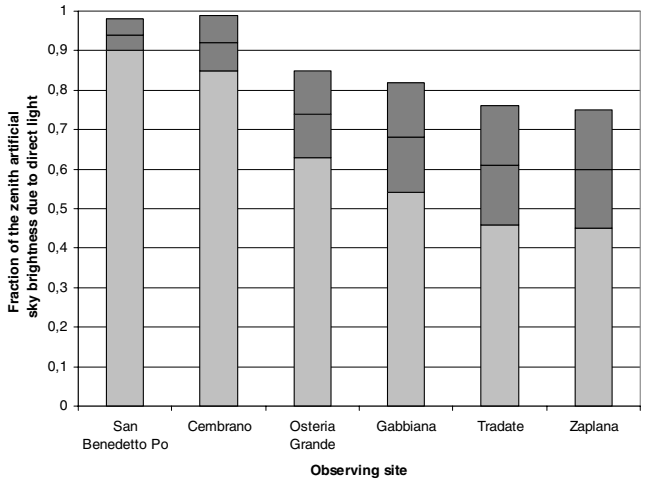

Figure 19. Evaluation of the fraction of artificial sky brightness as a result of direct light escaping from fixtures at six observing sites. The confidence intervals shown in dark grey are found by applying the propagation law for independent errors to the errors given in Table 4 and in the caption of Table 5.

most cases is less than the light reflected off the ground beneath the fixture. However, the sky brightness measured during snow events shows that the impact on the sky can be traced disproportionately to the 'small' fraction of direct uplight (Cinzano & Castro 2000; Luginbuhl, Walker & Wainscoat 2009). This shows that the total uplight flux is a very bad indicator of the sky pollution produced by outdoor lighting, a result already obtained theoretically by Cinzano & Castro (2000), Baddiley (2007) and Bessolaz (2009). A 'mere' 3 per cent of direct upward flux from fixtures produces far greater consequences on the sky far from the sources than the 10–20 per cent indirect flux reflected by the lighted terrain (roads, walkways, grass fields, buildings, etc.).

5 CONCLUSIONS

In this paper, we have presented the instruments, methods and some of the results of our campaign to measure sky brightness over the last 12 yr.

The sky brightness data can be displayed in all-sky maps, which allow us to see at a glance the sky quality and its contamination by artificial light.

The analysis of the time series has allowed us to identify a stop in the increase of artificial sky brightness at two sites protected by Italian regional laws against light pollution.

A comparison of the night sky brightness with and without snow coverage has given us proof that at the studied sites the sky brightness is more often, by far, a result of the direct light leaving upward from the fixtures rather than the light reflected by the terrain. This, in turn, has confirmed the technical prescription to use only fully shielded fixtures for external lighting, which allow zero uplight. By examining the effect of snow upon sky brightness, we can conclude that substantial reductions in light pollution are possible by using fully shielded lights.

The sky brightness measurements have already helped in calibrating the First World Atlas of Artificial Sky Brightness and the other maps based on satellite data published by our group. These measurements will also help in the calibration of forthcoming products and maps, and in testing and validating the new light propagation models being prepared by Cinzano. The low cost and the simplicity of the method described here should make portable CCDs more widely used for collecting a large amount of sky brightness data in standard photometric bands all over the world.

ACKNOWLEDGMENTS

I am grateful to the following: Giovanni Catanzaro of INAF – Osservatorio Astrofisico di Catania for his help and for kindly producing the All-Sky maps; Chad Moore of the United States National Park Service sky team for helpful hints and suggestions; Jan Hollan of Brno Observatory for the interesting discussions and ideas on the snow/no-snow measurements; Marco Comolli, Francesco Giubbilini, Andrej Mohar and Paolo Pescatori for the sky brightness data taken in difficult conditions after a snowstorm; Professor Roy Garstang for the valuable discussions and the stimulus he has given with his fundamental studies on light pollution. Part of this work has been supported by the University of Padua research project CPDG023488 headed by Pierantonio Cinzano. Calibration of some instruments was made at ISTIL with the support of Italian Space Agency contract I/R/160/02.

REFERENCES

Baddiley C., 2007, Towards Understanding Skyglow. Inst. Lighting Eng., Rugby, UK
Berry R., 1976, J. R. Astron. Soc. Canada, 70, 97
Bertiau F. C. S. J., de Graeve E. S. J., Treanor P. J. S. J., 1973, Vatican Obser. Publ., 1, 159
Bessel M. S., 1990, PASP, 102, 1181
Bessolaz N., 2009, http://astrosurf.com/licorness/dossiers%20PDF/control_PL_EN.pdf
Buil C., 1991, CCD Astronomy. Willmann-Bell, Richmond, VA, p. 267
Catanzaro G., Catalano F. A., 2000, Mem. Soc. Astron. Ital., 71, 211
Cinzano P., 1997, Inquinamento luminoso e protezione del cielo notturno. Istituto Veneto di Scienze, Lettere ed Arti, Venezia, p. 224
Cinzano P., 2000a, Mem. Soc. Astron. Ital., 71, 93
Cinzano P., 2000b, Mem. Soc. Astron. Ital., 71, 159
Cinzano P., 2003, in Schwarz H. E., ed., Light Pollution: The Global View. Kluwer Academic, Dordrecht
Cinzano P., 2005, Night Sky Photometry with Sky Quality Meter, ISTIL Internal Report, 9
Cinzano P., Castro J. D., 2000, Mem. Soc. Astron. Ital., 71, 251
Cinzano P., Falchi F., 2003, Mem. Soc. Astron. Ital., 74, 458
Cinzano P., Falchi F., Elvidge C. D., 2000, MNRAS, 318, 641
Cinzano P., Falchi F., Elvidge C. D., 2001a, MNRAS, 328, 689
Cinzano P., Falchi F., Elvidge C. D., 2001b, MNRAS, 323, 34
Duriscoe D. M., Luginbuhl C. B., Moore C. A., 2007, PASP, 119, 192
ESA 1997, The Hipparcos and Tycho Catalogues, ESA SP-1200
Falchi F., 1999, Master's thesis, Milan Univ., Milan
Falchi F., Cinzano P., 2000, Mem. Soc. Astron. Ital., 71, 139
Favero G., Federici A., Blanco A. R., Stagni R., 2000, Mem. Soc. Astron. Ital., 71, 223
Garstang R. H., 1984, The Observatory, 104, 196
Garstang R. H., 1986, PASP, 98, 364
Garstang R. H., 1987, in Mills R. L., Franz O. G., Abels H. D., eds, Identification, Optimization and Protection of Optical Observatory Sites. Lowell Observatory, Flagstaff, p. 199
Garstang R. H., 1989, PASP, 101, 306
Garstang R. H., 1991, PASP, 103, 1109
Garstang R. H., 2004, The Observatory, 124, 14
Isobe S., Hamamura S., 1999, in Isobe S., Hamamura S., eds, ASP Conf. Ser. Vol. 139, Preserving the Astronomical Windows. Astron. Soc. Pac., San Francisco, p. 191
Hanel A., 2000, Mem. Soc. Astron. Ital., 71, 153

Herold M., Roberts D., 2005, Appl. Opt., 44, 4327
Hoag A. A., 1973, PASP, 85, 503
Hoffleit D., Warren W. H., Jr, 1991, The Bright Star Catalogue V, revised edn. Yale Univ. Obs., New Haven, CT
Johnson H. L., 1963, in Basic Astronomical Data. Univ. Chicago Press, Chicago, p. 209
Kalinowski J. K., Roosen R. G., Brandt J. C., 1975, PASP, 87, 869
Krisciunas K., 1990, PASP, 102, 1052
Krisciunas K., Semler R. D., Richards J., Schwarz E. H., Suntzeff B. N., Vera S., Sanhueza P., 2007, PASP, 119, 687
Luginbuhl C. B., Walker C. E., Wainscoat R. J., 2009, Phys. Today, 62, 35
Patat F., 2003, A&A, 400, 1183
Patat F., 2008, A&A, 481, 575
Piersimoni A., Di Paolantonio A., Brocato E., 2000, Mem. Soc. Astron. Ital., 71, 221
Rabaza O., Galadi-Enriquez D., Espin Estrella A., Aznar Dols F., 2010, J. Environ. Management, 91, 1278
Regione Lombardia, 2003, http://62.101.84.24/OSIEG/AreaEnergia/contenuti_informativi/contenuto_informativo_Energia.shtml?586
Walker M. F., 1970, PASP, 82, 672
Walker M. F., 1973, PASP, 85, 508
Walker M. F., 1988, PASP, 100, 496
Walker M. F., 1991, in Crawford D. L., ed., ASP Conf. Ser. Vol. 17, Light Pollution, Radio Interference and Space Debris. Astron. Soc. Pac., San Francisco, p. 52
Zitelli V., 2000, Mem. Soc. Astron. Ital., 71, 193

This paper has been typeset from a Microsoft Word file prepared by the author.